Mol Neurobiol
DOI 10.1007/s12035-016-9850-1

C9ORF72 Regulates Stress Granule Formation and Its Deficiency Impairs Stress Granule Assembly, Hypersensitizing Cells to Stress

Niran Maharjan[1,2] · Christina Künzli[1] · Kilian Buthey[1] · Smita Saxena[1]

Received: 16 November 2015 / Accepted: 9 March 2016

Abstract Hexanucleotide repeat expansions in the C9ORF72 gene are causally associated with frontotemporal lobar dementia (FTLD) and/or amyotrophic lateral sclerosis (ALS). The physiological function of the normal C9ORF72 protein remains unclear. In this study, we characterized the subcellular localization of C9ORF72 to processing bodies (P-bodies) and its recruitment to stress granules (SGs) upon stress-related stimuli. Gain of function and loss of function experiments revealed that the long isoform of C9ORF72 protein regulates SG assembly. CRISPR/Cas9-mediated knockdown of C9ORF72 completely abolished SG formation, negatively impacted the expression of SG-associated proteins such as TIA-1 and HuR, and accelerated cell death. Loss of C9ORF72 expression further compromised cellular recovery responses after the removal of stress. Additionally, mimicking the pathogenic condition via the expression of hexanucleotide expansion upstream of C9ORF72 impaired the expression of the C9ORF72 protein, caused an abnormal accumulation of RNA foci, and led to the spontaneous formation of SGs. Our study identifies a novel function for normal C9ORF72 in SG assembly and sheds light into how the mutant expansions might impair SG formation and cellular-stress-related adaptive responses.

Electronic supplementary material The online version of this article (doi:10.1007/s12035-016-9850-1) contains supplementary material, which is available to authorized users.

✉ Smita Saxena
smita.saxena@izb.unibe.ch

[1] Institute of Cell Biology, University of Bern, Baltzerstrasse 4, 3012 Bern, Switzerland

[2] Graduate School for Cellular and Biomedical Sciences, University of Bern, Bern, Switzerland

Keywords C9ORF72 · ALS · Motor neuron degeneration · Stress granules · Cell recovery

Introduction

Amyotrophic lateral sclerosis (ALS) or motor neuron disease (MND) and frontotemporal lobar dementia (FTLD) are devastating neurodegenerative diseases of as yet unknown etiology and pathogenesis. ALS is characterized by the progressive and selective loss of motor neurons in the brain and spinal cord. The majority of ALS cases (90 %) are sporadic, and in approximately 10 % of cases, the disorder is dominantly inherited. The disease is characterized by the degeneration of motor neurons leading to muscle wasting, paralysis, and death usually within 2–3 years of symptom onset due to respiratory failure [1]. In contrast, FTLD comprises about 50 % of dementia cases appearing before 65 years of age [2] and is characterized by the selective degeneration of neurons within the frontal and temporal lobes of the brain leading to progressive behavioral and personality alterations together with semantic dementia [3]. Both ALS and FTLD are accepted as multisystem diseases wherein up to 50 % of ALS patients can show some degree of impairment in the frontotemporal area involving cognition [4, 5] and conversely 16 % of FTLD patients develop motor neuron dysfunction suggesting that both these diseases belong to a group of diseases sharing clinical and pathological aspects [6].

The notion that ALS and FTLD represent the two ends of the same spectrum of disease is strongly supported by the discovery of mutations within the TAR DNA binding protein 43 (TDP-43) as being causally linked with sporadic and with dominant inherited forms of ALS as well as FTLD. This suggested shared aspects of cellular and molecular vulnerability within the two regions of the central nervous system (CNS) [7, 8]. Furthermore, the observation that TDP-43 and fused in

Published online: 01 April 2016

sarcoma (FUS)/translocated in liposarcoma protein (TLS) are present as pathological inclusions in the vast majority of superoxide dismutase 1 (SOD1)-negative ALS cases as well as in subtypes of FTLD, strengthened this concept of ALS and FTLD belonging to the same clinical spectrum of disease.

Recently, hexanucleotide repeat expansion in the C9ORF72 gene was identified in patients with a combined ALS/FTLD phenotype, thereby confirming the genetic and clinical overlap between these two diseases. Mutations in C9ORF72 gene presently remain as the most common mutation to be identified which is associated with FTLD and/or ALS. A considerable effort has been put in understanding the pathological mechanism associated with the expanded *C9ORF*72 gene. Initial studies revealed a reduction in the messenger RNA (mRNA) levels of some C9ORF72 variants in ALS, suggesting a loss-of-function mechanism [9–12]. Besides, it was shown that the transcripts containing the hexanucleotide repeat expansion could accumulate within the nucleus forming toxic RNA foci [10]. Presently, several studies have reported that the repeat-associated non-ATG (RAN) translation of the hexanucleotide expansion produces dipeptide repeat proteins which forms neuronal inclusions and serves as a pathological hallmark of the disease [13, 14]

The normal physiological function of C9ORF72 protein remains as yet unclear and under-characterized despite the widespread expression of C9ORF72 mRNA in CNS [9]. A recent study has shown that the endogenous C9ORF72 is involved in intracellular trafficking between endosomal and lysosomal subcompartments and is associated with Rab proteins in neuronal cell lines [15]. However, the precise regulatory role of the various C9ORF72 isoforms in neurons, and how the impairment of this function due to the hexanucleotide repeat expansion might relate to other cellular pathways implicated in ALS pathogenesis, remain unclear. Here, using primary cortical neurons and immortalized mouse neuroblastoma (n2a) and human SK-N-MC cells, we show that despite the large majority of endogenous C9ORF72 being nuclear, a fraction of the protein is localized in processing bodies (P-bodies). C9ORF72 colocalized with stress granules (SGs) in diverse cell lines in response to cellular stressors such as endoplasmic reticulum (ER) stress or heat shock. Functionally, the long isoform of C9ORF72 selectively regulated SG assembly upon stress, and the overexpression of this isoform led to the spontaneous appearance of SGs. In contrast, the short isoform of C9ORF72 protein was not involved in SG formation, thereby hinting toward differential physiological functions of the various C9ORF72 isoforms. Conversely, the knockdown of C9ORF72 via CRISPR/Cas9 completely inhibited SG assembly during cellular stress response and compromised cell recovery and survival. Importantly, the transient expression of C9ORF72 carrying the pathogenic hexanucleotide repeat expansion led to impaired expression of the C9ORF72 protein, accumulation of nuclear and cytoplasmic RNA foci, presence of toxic dipeptide repeat proteins, and spontaneous induction of SGs. Our data demonstrates a function for C9ORF72 in SG assembly and provides evidence as to how the hexanucleotide expansion might interfere with C9ORF72 expression and SG formation, simultaneously inducing cellular stress due to the formation of toxic RNA foci and dipeptide repeat proteins, thereby impairing cellular recovery capacity and survival.

Experimental Procedures

Plasmids

Human cDNA constructs for C9ORF72 (Myc-DDK-tagged), transcript variant 1 (C9(SF) myc) (RC222418), and C9ORF72 (Myc-DDK-tagged), transcript variant 2 (C9(LF) myc) (RC209700), were purchased from Origene. CRISPR/Cas9 KO plasmid (sc-428521) against mouse C9ORF72 was purchased from Santa Cruz Biotechnology. EGFP construct containing hexanucleotide repeat expansion [16] was a generous gift from Prof. Peng Jin (Dept. of Human Genetics, Emory University School of Medicine). Hexanucleotide repeat expansion was subcloned into C9(LF) myc plasmid in between CMV promoter and ATG start site using EcoRI and KpnI restriction enzymes. Sequence and size of repeat were verified by sequencing and restriction digestion.

Cell Culture

Mouse neuroblastoma cells (n2a) from ATCC were maintained in Dulbecco modified Eagle medium (DMEM) containing 10 % (*v*/*v*) fetal bovine serum, 1 % (*v*/*v*) penicillin, and streptomycin solution and kept at 37 °C in 5 % CO_2. Cells were plated 24 h before transfection. Transfections were carried out using TransIT-Neural transfection reagent (Mirus) according to manufacturer protocol. Transfected cells were incubated for 48 h to allow transient expression of protein.

Primary cortical neurons were prepared from embryonic brains (E17) of mice. Meninges were removed and the cortical neurons were separated by mechanical dissociation and mild trypsinization. Cells were plated at a density of 2×10^5 cells/well (12-well plates) and 5×10^6 cells/well (6-well plates) on poly-D-lysine-precoated glass coverslips. Neurobasal medium (Invitrogen) supplemented with 1.2 mM glutamine, and 2 % (*v*/*v*) B27 supplement (Invitrogen; 20 ml/l) was used as a culture medium. After 72 h, neurons were treated with 3 mM dithiothreitol (DTT) for 2 h or incubated at 45 °C for 30 min for stress experiment. Transfection of cortical neuron was carried out using Lipofectamine 2000 Transfection reagent (Thermo Fisher Scientific) according to manufacturer protocol.

Fluorescence-Activated Cell Sorting

For fluorescence-activated cell sorting (FACS) sorting, n2a cells were transiently transfected with CRISPR/Cas9 plasmid

targeting 5′-UTR of mouse C9ORF72 (C9-CRISPR) for 48 h, then trypsinized and resuspended in HBSS containing 2 % serum. C9ORF72 knockout cells were then sorted using ARIA III (BD Biosciences) based on GFP expression. Non-transfected n2a cells were used as negative control for FACS sorting. Proteins from FACS sorted cells were extracted using RIPA buffer.

Cell Death Assay and Treatment

In order to evaluate cell viability, a trypan blue exclusion assay was performed as previously described [17]. Cell counts were determined in duplicate from three separate experiments. For SG formations, either cells were treated with 3 mM DTT or incubated at 45 °C for 30 min. To analyze the recovery of cells after stress, DTT containing medium were washed off after 2 h of DTT treatment, and cells were incubated in normal medium for 1 or 2 h. To evaluate cell viability in cortical neurons, propidium iodide (PI) exclusion assay was used. In short, transfected cortical neurons were washed with phosphate-buffered saline (PBS) and then incubated at room temperature for 5 min in PBS containing 20 μg/ml PI. The staining solution was then removed and PBS was added. Cells were then analyzed using a fluorescent microscope.

Immunoblotting

Cells were lysed in RIPA buffer containing 50 mM Tris (pH 8), 150 mM NaCl, 0.5 % sodium deoxycholate, 1 % Triton X-100, 0.1 % sodium dodecyl sulphate (SDS), and Protease Inhibitor (Roche). Protein concentrations were determined using Pierce BCA protein assay kit (Thermo Fischer Scientific) according to manufacturer protocol. Proteins were denatured at 95 °C for 5 min with Laemmli sample buffer containing β-mercaptoethanol. Proteins were then separated on a 10 % SDS-PAGE gel, transferred to polyvinylidenedifluoride (PVDF) membrane, and blocked in 5 % milk made in PBS with 0.1 % Tween for 1 h. For immunoblotting primary antibodies used were: rabbit anti-C9ORF72 (Proteintech, 22637-1-AP; 1:1000), mouse anti-GAPDH (Acris, ACR001P; 1:5000), mouse anti-Tubulin (Sigma Aldrich, T5168; 1:5000), goat anti-TIA-1 (Santa Cruz, sc-1751; 1:1000), goat anti-HuR (Santa Cruz, sc-5483; 1:1000), mouse anti-TDP-43 (Abcam, ab104223; 1:2500), mouse anti-FUS/TLS (Santa Cruz, sc-47711; 1:1000), mouse anti-DCP1a (Santa Cruz, sc-100706; 1:1000), goat anti-G3BP1 (Santa Cruz, sc-70283; 1:1000), and rabbit anti-C9RANT antibody (Novus Biologicals; 1:1000), were incubated overnight at 4 °C. Horseradish peroxidase (HRP)-conjugated secondary antibodies (goat anti-mouse IgG HRP (Santa Cruz, sc-2005; 1:10000), goat anti-rabbit IgG HRP (Santa Cruz, sc-2004; 1:10,000), and donkey anti-goat IgG HRP (Santa Cruz, sc-2020; 1:10000)), were incubated for 1 h at room temperature, washed, and developed using ECL system.

Immunofluorescence

For immunofluorescence, n2a cells or cortical neurons were plated on poly-D-lysine-coated coverslips. Cells were fixed using 4 % paraformaldehyde (PFA) for 15 min and blocked for 1 h using 3 % bovine serum albumin (BSA) and 0.1 % TritonX-100 in PBS and were incubated with primary antibody (rabbit anti-C9ORF72 (Proteintech, 22637-1-AP; 1:500), goat anti-TIA-1 (Santa Cruz, sc-1751; 1:100), goat anti-HuR (Santa Cruz, sc-5483; 1:100), mouse anti-TDP-43 (Abcam, ab104223; 1:1000), mouse anti-FUS/TLS (Santa Cruz, sc-47711; 1:1000), mouse anti-GW182 antibody (Santa Cruz, sc-56314; 1:25) mouse anti-DCP1a (Santa Cruz, sc-100706; 1:100), and goat anti-G3BP1 (Santa Cruz, sc-70283; 1:100)) overnight at 4 °C. Cells were washed three times with PBS and incubated with Alexa Fluor (488/568/647) fluorescently labeled secondary antibodies and DAPI in blocking buffer for 1 h at room temperature, and then washed three times before mounting on slides using mowiol (Hoechst). Images were acquired with a confocal microscope Olympus FluoView^{TM} FV1000 (Olympus) with 60× silicon objective. Images were later processed using Imaris 7.6 (Bitplane). For SG formations, images were taken from different areas of the coverslips and the total number of transfected cells together with cells showing cytoplasmic aggregates for TIA-1 were counted. The ratio was calculated and representative images from three to five independent experiments are shown. The number of SGs was counted manually but blind using ImageJ.

Fluorescent In Situ Hybridization

Cy3-labeled C4G2 probes were synthesized by Microsynth and used as antisense probes. Cells were fixed in ice-cold 4 % PFA for 15 min and washed three times with PBS. Cells were incubated with 70 % ethanol overnight at 4 °C. The next day, cells were rehydrated in PBS for 20 min and blocked with 3 % BSA + 0.2 % Triton X-100 for 1 h at room temperature. Following this, the coverslips were incubated in prehybridization solution (50 % formamide, 2× SSC (Saline Sodium Citrate)) for 15 min at room temperature. Cells were hybridized overnight at 37 °C with probe (1 μM) in 50 % formamide, 10 % dextransulfate, 2× SSC, and RNAse inhibitor in a dark humid chamber made with papers soaked in 50 % formamide/2× SSC. Cells were washed three times in 50 % formamide in 2× SSC for 5 min each at 42 °C. DNA was counterstained using DAPI (5 min in 2× SSC). Cells were later washed two times with 2× SSC and then mounted on coverslips.

RNA Extraction, Quantitative Real-Time PCR, and Primers

RNA was extracted from n2a cells using TRIzol (Invitrogen) as manufacturer protocol. Reverse transcription was performed with the AffinityScript Multiple Temperature Reverse Transcriptase Kit (Agilent Technologies). qPCR was performed with KAPA SYBR FAST qPCR Kit (KAPA Biosystems) using a Rotor-Gene Q (Qiagen). RNA levels were normalized to tubulin, and gene differences were quantified with the comparative CT method. The following primers were used:

For TIA-1: forward 5′-CAGTTCCCATGAAAG TGCAGC-3′,
reverse 5′-CCACATGCCCTTCAATGGTAGTA-3′
For tubulin: forward 5′-CCGCGAAGCAGCAACCAT-3′,
reverse 5′-CCAGGTCTACGAACACTGCC-3′
For HuR: forward 5′-GGATGACATTGGG AGAACGAAT-3′,

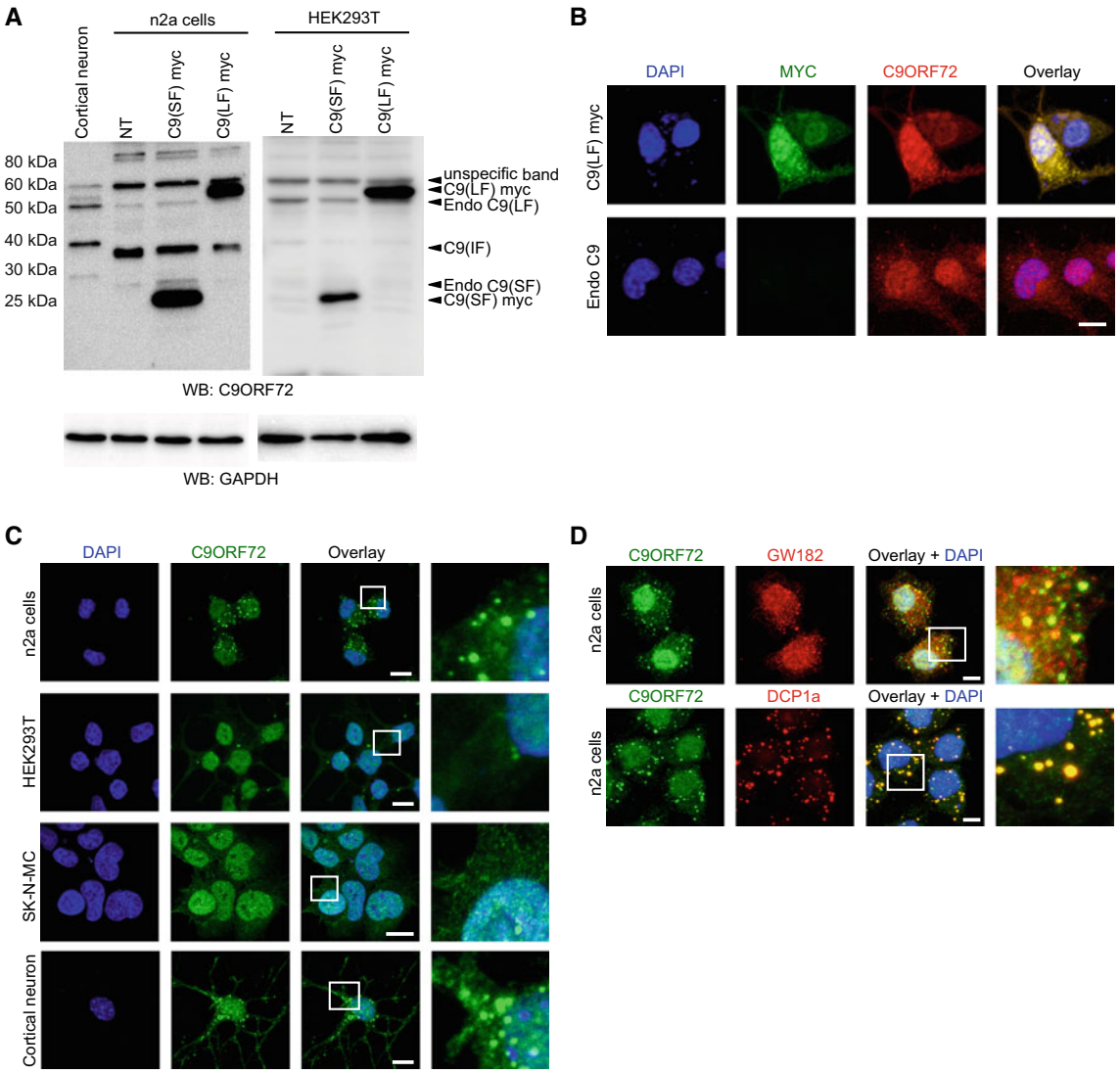

Fig. 1 C9ORF72 antibody specificity and expression pattern in different cell lines and cortical neurons. **a** n2a and HEK293T cell lines were transfected with either the myc-tagged long-isoform of C9ORF72 (C9(LF) myc) or myc-tagged short-isoform of C9ORF72 (C9(SF) myc) constructs, and proteins were extracted from transfected as well as non-transfected cells and from mouse cortical neuronal cultures. Western vblotting was done with C9ORF72 antibody from Proteintech. Along with the overexpressed protein, a faint band presents for endogenous C9ORF72 protein at 50 kDa (C9(LF)) and 25 kDa (C9(SF)) as expected. An additional band of 37 kDa (C9(IF)) was observed in mouse n2a cell lines but was absent in human HEK293T cells. Representative blot from four experiments. **b** n2a cells transfected with C9(LF) myc was immunostained with myc antibody and C9ORF72 antibody and both immunoreactivity strongly overlapped suggesting that the antibody detects C9ORF72 in its native configuration. **c** C9ORF72 is expressed mainly in the nucleus together with a diffused staining pattern in the cytoplasm. Distinct C9ORF72-positive cytoplasmic puncta were found in neuronal cell lines and primary cortical neurons. Note the presence of these puncta along neurites in a cortical neuron. **d** Cytoplasmic puncta immunoreactive for C9ORF72 were also positive for GW182 and DCP1a, which are markers for processing bodies (P-bodies) (*scale bar* = 4 μm for all image panels)

reverse 5′-TGTCCTGCTACTTTATCCCGAA-3′.
For C9ORF72: forward 5′-GCGGCTACCTTTGCTTA CTG-3′,
reverse 5′-GCACTTGGTCTGTCTTTGGAG-3′.

Statistical Analysis

Data are presented as mean ± SEM. Statistical analysis was performed using a two-tailed Student's *t* test and GraphPad

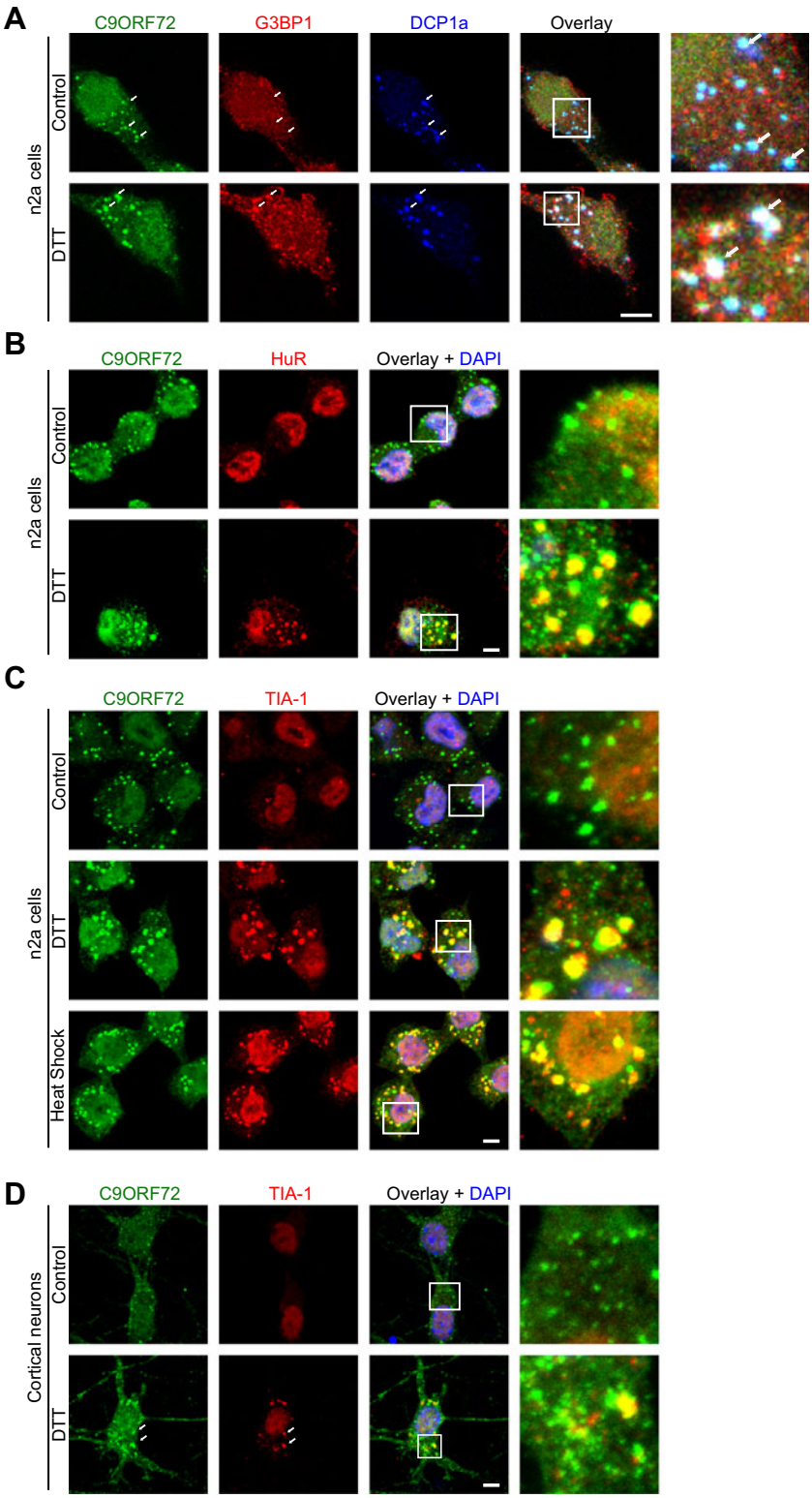

Fig. 2 C9ORF72 localizes to stress granules in mammalian cells and primary cortical neurons. **a** Treatment of n2a cells with 3 mM DTT for 2 h resulted in the localization of C9ORF72 to G3BP1 positive stress granules (SGs) which were also positive for DCP1a. **b** A second SG marker, HuR, also confirmed the localization of C9ORF72 to SGs after DTT treatment. **c** Not only DTT but also heat shock resulted in the localization of C9ORF72 with TIA-1 positive SGs. **d** C9ORF72 also localizes with TIA-1-positive SGs in primary neurons after DTT treatment (*scale bar* = 4 μm for all image panels)

Prism 5 software (GraphPad Software, Inc.). Statistically significant p values were those lower than 0.05 and are marked by an asterisk.

Results

C9ORF72 Is Mainly Localized Within the Nucleus and P-Bodies

As several studies had previously mentioned the issue of non-specificity of C9ORF72 antibody [18], we started this study by validating the specificity of the C9ORF72 antibody from Proteintech for both native and denatured protein. Western blotting of lysates from primary cortical neurons, n2a cells, and HEK293T cells notably detected a band at approximately 48 and 25 kDa along with the mouse specific 37-kDa isoform present in n2a cells (termed intermediate form; C9(IF)) but absent in human HEK293T cells. In parallel, lysates from n2a cells and HEK293T cells transiently expressing either the full-length myc-tagged C9ORF72 abbreviated as (C9(LF) myc) or the shorter form of C9ORF72 (C9(SF) myc) were detected along with the endogenous C9ORF72 by this antibody (Fig. 1a). Further, transfection of n2a cells with C9(LF) myc revealed a strong overlap of immunoreactivities for myc and C9ORF72 (Fig. 1b), indicating that the antibody can detect native protein. We next immunostained various neuronal cell lines such as n2a, SK-N-MC, and non-neuronal HEK293T cells to examine the expression pattern of C9ORF72. In all cell lines, C9ORF72 exhibited both nuclear and cytoplasmic localization and the cytoplasmic proportion of C9ORF72 often presented vesicular appearance (Fig. 1c). Similar localization pattern of C9ORF72 was observed in primary cortical neurons. Interestingly, C9ORF72 was also enriched within neuronal processes (Fig. 1c, zoom). To elucidate the identity of the cytoplasmic vesicular structures, we hypothesized that C9ORF72-positive cytoplasmic puncta might be P-bodies. Using specific markers against P-bodies, GW182 and DCP1a, a high degree of overlap between the two markers and C9ORF72 was observed. As DCP1a expression is largely confined to P-bodies and nearly 100 % of DCP1a-positive cytoplasmic puncta were also positive for C9ORF72, this confirmed that a fraction of C9ORF72 resides within P-bodies (Fig. 1d).

C9ORF72 Associates with SGs in Cells and Primary Cortical Neurons upon Cellular Stress

As a functional interplay between P-bodies and stress granules (SGs) is well described [19, 20], we further examined whether C9ORF72 would colocalize with SGs under stress conditions. To induce the formation of SGs, we treated n2a cells with dithiothreitol (DTT) for 2 h or heat-shocked the cells at 45 °C for 30 min and fixed the cells. Upon stress, SGs (G3BP1 immunopositive) were formed within the cytoplasm that were also strongly immunopositive for C9ORF72. Interestingly in control condition, negligible overlap between P-bodies marker DCP1a and SG marker G3BP1 was observed and C9ORF72 immunopositive puncta were mainly associated with P-bodies. However, stress-induced SGs were immunopositive for all three components, suggesting that SGs, P-bodies, and C9ORF72 physically interact with one another in vivo (Fig. 2a). To further confirm the identity of cellular structures to which C9ORF72 localized upon stress induction are SGs, additional colocalization studies with

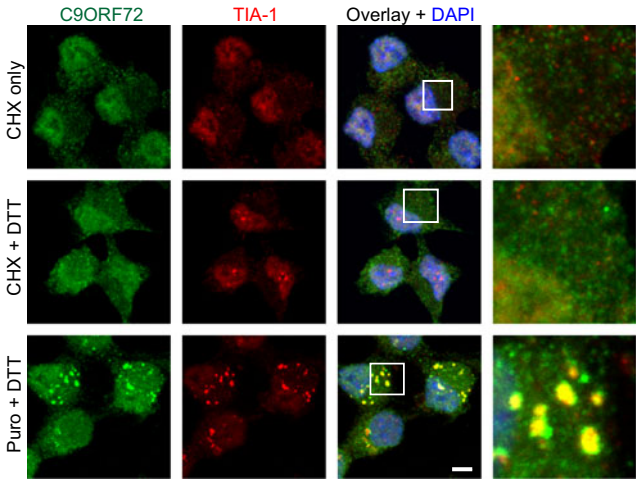

Fig. 3 C9ORF72 are specific to SGs. Treatment of cells with cycloheximide (CHX) (inhibits SG assembly by maintaining polysomes, preventing free mRNA from accumulating in the cytoplasm) alone for 2 h led to the dissociation of C9ORF72-positive cytoplasmic puncta in control cells. Despite DTT treatment for 2 h, cells were unable to assemble SGs in the presence of cycloheximide. Treatment of cells with puromycin (Puro) (stimulates the formation of SGs by dissociating polysome and producing free mRNA in cytoplasm) and DTT together for 2 h led to the formation of C9ORF72-positive puncta which colocalized with TIA-1-positive SGs (*scale bar* = 4 μm for all image panels)

Fig. 4 C9ORF72 overexpression causes spontaneous formation of SGs. ▶ **a** Overexpression of C9(LF) myc in n2a cells led to spontaneous formation of SGs (marked with TIA-1) in approximately 75 % of the transfected cells as compared to control GFP-transfected cells. **b** Overexpression of C9(LF) myc also led to the formation of TIA-1-positive SGs in primary cortical neurons. **c** n2a cells transfected with C9(LF) myc were treated with 3 mM DTT for 30 min, 1 h, 2 h, or 3 h and stained for TIA-1 to measure SG assembly kinetics in the presence of DTT. **d** To measure SG disassembly kinetics, n2a cells transfected with C9(LF) myc were treated with DTT for 3 h, followed by DTT removal, addition of fresh medium, reincubation of cells for 30 min, 1.5 h, or 3 h, and followed by cell fixation and staining for TIA-1. **e** Significant differences in the number of SGs assembled were observed only after 30 min of DTT treatment. Quantitative analysis revealed significant differences in the number of SGs formed for the non-treated and the DTT-treated (30 min) conditions. Each value represents the mean ± SEM of 25 cells from three independent experiments, $*p<0.05$, $**p<0.01$ (*scale bar* = 4 μm for all image panels)

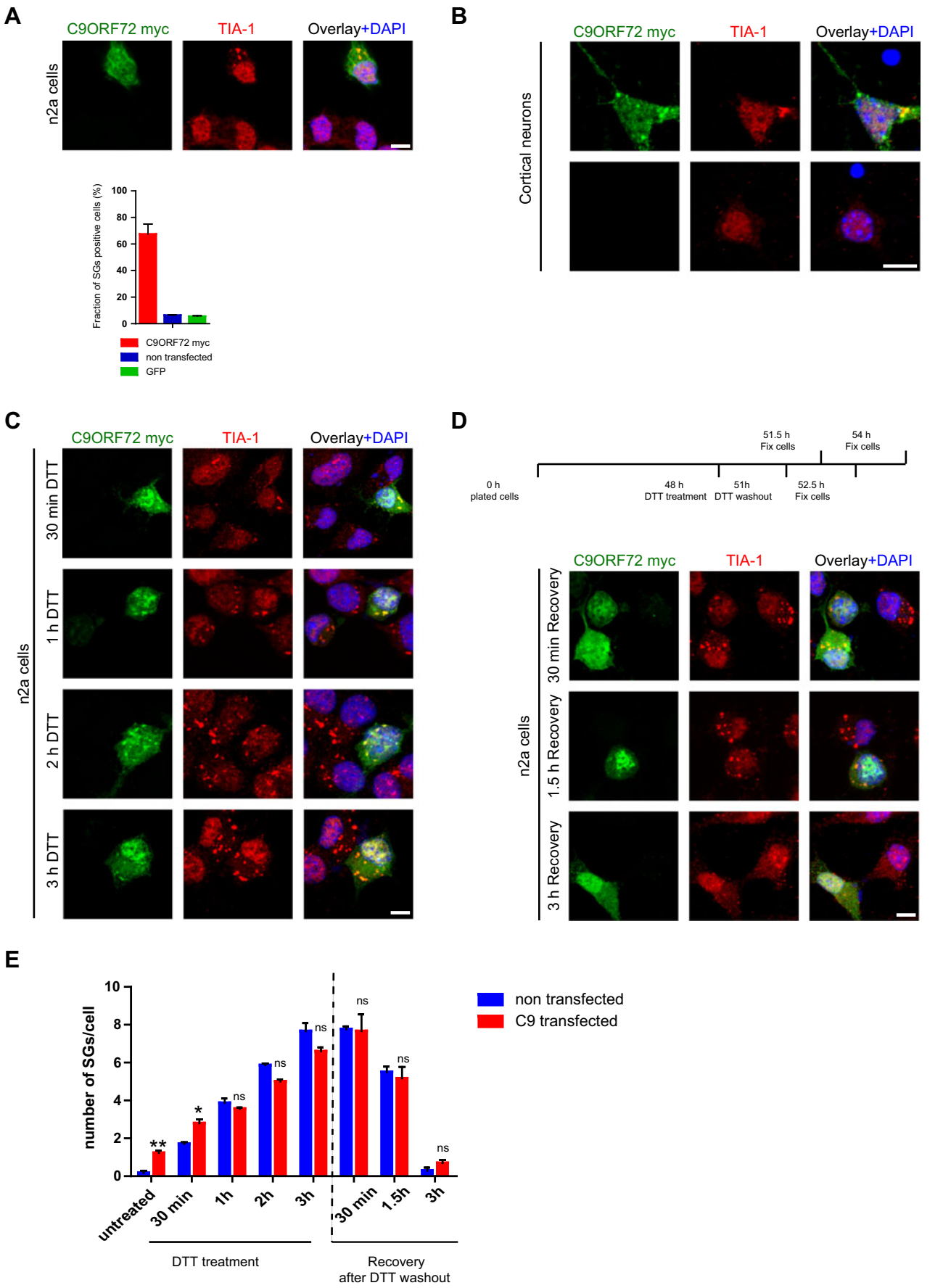
A
C9ORF72 myc
TIA-1
Overlay+DAPI
n2a cells
Fraction of SGs positive cells (%)
100
80
60
40
20
0
C9ORF72 myc
non transfected
GFP
B
C9ORF72 myc
TIA-1
Overlay+DAPI
Cortical neurons
C
C9ORF72 myc
TIA-1
Overlay+DAPI
n2a cells
30 min DTT
1 h DTT
2 h DTT
3 h DTT
D
51.5 h
Fix cells
54 h
Fix cells
0 h
plated cells
48 h
DTT treatment
51h
DTT washout
52.5 h
Fix cells
C9ORF72 myc
TIA-1
Overlay+DAPI
n2a cells
30 min Recovery
1.5 h Recovery
3 h Recovery
E
number of SGs/cell
10
8
6
4
2
0
**
*
ns
ns
ns
ns
ns
ns
untreated
30 min
1h
2h
3h
30 min
1.5h
3h
DTT treatment
Recovery
after DTT washout
non transfected
C9 transfected

another well-known marker for SGs, Hu-antigen R (HuR), were performed [21]. As expected, nearly all the SGs formed under stress were strongly positive for both HuR and C9ORF72, demonstrating that upon elevated stress, cytoplasmic C9ORF72 preferentially localizes with SGs, and that normal C9ORF72 is a novel SG component (Fig. 2b). A similar response was also observed with yet another SG marker; T-cell-restricted intracellular antigen-1 (TIA-1), after cells were heat-shocked at 45 °C. The size of the SGs formed was slightly smaller and more numerous compared to those SGs formed after DTT treatment, most likely reflecting the difference in the duration of stress (Fig. 2c). To exclude the possibility that the observed response was cell line specific and not physiological, we expanded our analysis to primary cortical neurons which were treated with DTT for 60 min, leading to the formation of SGs positive for C9ORF72 (Fig. 2d).

To further test whether these cytoplasmic puncta are indeed SGs, the cells were treated with cycloheximide (CHX) to block the formation of DTT-induced SGs [22]. Indeed, the cotreatment of n2a cells with CHX and DTT blocked the formation of TIA-1-C9ORF72-positive SGs (Fig. 3). In the same line, cotreatment of cells with DTT and puromycin, a drug that actively dismantles polysomes thereby promoting the formation SGs, led to the enhanced formation of SGs which were all positive for C9ORF72 (Fig. 3). These experiments provide evidence that upon cellular stress, C9ORF72-positive cytoplasmic puncta actively associate with SGs.

C9ORF72 Overexpression Causes Spontaneous Formation of SGs

Since a role for normal C9ORF72 in SG assembly has not been reported, we next addressed whether C9ORF72 levels would per se impact the process of SG formation and dynamics. Approximately 75 % of cells transfected with C9(LF) myc exhibited spontaneous SGs in the absence of stress as observed by the presence of cytoplasmic TIA-1-positive structures (Fig. 4a). In GFP-overexpressing cells, only around 5 % of cells exhibited spontaneous SGs indicating that high levels of C9ORF72-induced spontaneous SG formation. Similar response was also observed in cortical neurons where overexpression of C9(LF) myc led to the spontaneous formation of SGs even in the absence of cellular stress (Fig. 4b). Next, we examined whether increased C9ORF72 levels would alter the assembly or the disassembly rate of SGs in response to stress. In order to measure the SG assembly kinetics, cells were transfected with C9(LF) myc and treated with DTT for 30 min, 1 h, 2 h, or 3 h followed by fixation and immunostaining for myc and TIA-1 (Fig. 4c). To measure SG disassembly kinetics, cells were treated with DTT for 3 h leading to robust amounts of SG induction in both transfected and untransfected cells, followed by DTT washout and a recovery period of 30 min, 1.5 h, or 3 h (Fig. 4d). In the case of SG assembly, the number of SGs formed after 30 min DTT treatment within myc immunopositive versus myc negative cells was 1.5-fold higher but, over time, no significant difference was observed in the SG numbers after DTT treatment. Similarly, DTT washout experiments revealed that the rate of SG disassembly after removal of stressor DTT remained unaltered between C9(LF) myc overexpressing and control cells (Fig. 4e). These experiments demonstrate that overall C9ORF72 levels do not determine or influence the kinetics of SG assembly and disassembly.

Fig. 5 C9ORF72 is needed for SG formation. **a** n2a cells transiently transfected with C9-CRISPR were FACS sorted after 48 h of transfection; total protein was extracted using RIPA buffer. Western blotting revealed a decline in C9ORF72 protein levels for all isoforms by almost 80 % compared to control cells. The quantification for C9ORF72 reduction was calculated from three independent FACS sorting experiments and quantification of the expression intensity is the mean of three experiments, *$p<0.05$, **$p<0.01$, ***$p<0.001$. **b** n2a cells transfected with either C9-CRISPR or GFP plasmid for 48 h were stained for SG marker, TIA-1 with or without DTT treatment. C9-CRISPR-transfected cells failed to make SGs (*arrow*) whereas adjacent GFP-transfected cells were positive for SGs. **c** The number of dead cells was counted using trypan blue solution in untransfected, GFP-transfected, and C9-CRISPR-transfected cells after 0, 2, and 4 h of DTT treatment. Results shown are mean ± SEM from three independent experiments. **$p<0.01$. **d** After 2 h of DTT treatment, cells were left to recover in normal DMEM medium for 1 and 2 h and the number of dead cells was counted. Results shown are mean ± SEM from three independent experiments. *$p<0.05$ **$p<0.01$. **e**, **f** n2a cells double transfected with C9-CRISPR and C9(LF) myc or C9(SF) myc plasmid were treated with DTT and then stained for TIA-1 (*arrows*). Approximately 82 % of C9-CRISPR cells transfected with C9(LF) myc were able to make SGS whereas only 20 % of C9-CRISPR cells transfected with C9(SF) myc were positive for SGs after DTT treatment as compared to GFP transfected control cells where nearly 95 % of cells were SG-positive. Each value represents the mean ± SEM of 25 cells each from three independent experiments, ***$p<0.001$ (*scale bar* = 4 μm for all image panels)

C9ORF72 Is Required for SG Formation

Subsequently, a knockdown of C9ORF72 was performed by using C9ORF72-specific CRISPR/Cas9 (C9-CRISPR). As GFP is integrated to indicate successful knockdown, GFP-positive cells were FACS sorted and C9ORF72 protein levels were measured via western blotting. A reduction of nearly 75 % was consistently achieved for all isoforms of C9ORF72 from three different FACS sorting experiments (Fig. 5a). After having established the successful knockdown of C9ORF72, we next examined the fate of SGs after DTT treatment. The loss of C9ORF72 expression inhibited SG formation although neighboring untransfected cells exhibited robust SGs in the presence of DTT (Fig. 5b). As SG assembly requires eIF2alpha phosphorylation, we examined its phosphorylation status and found that GFP-positive C9-CRISPR cells exhibited significantly low amounts of phosphorylated eIF2alpha in the presence of DTT as compared to C9-

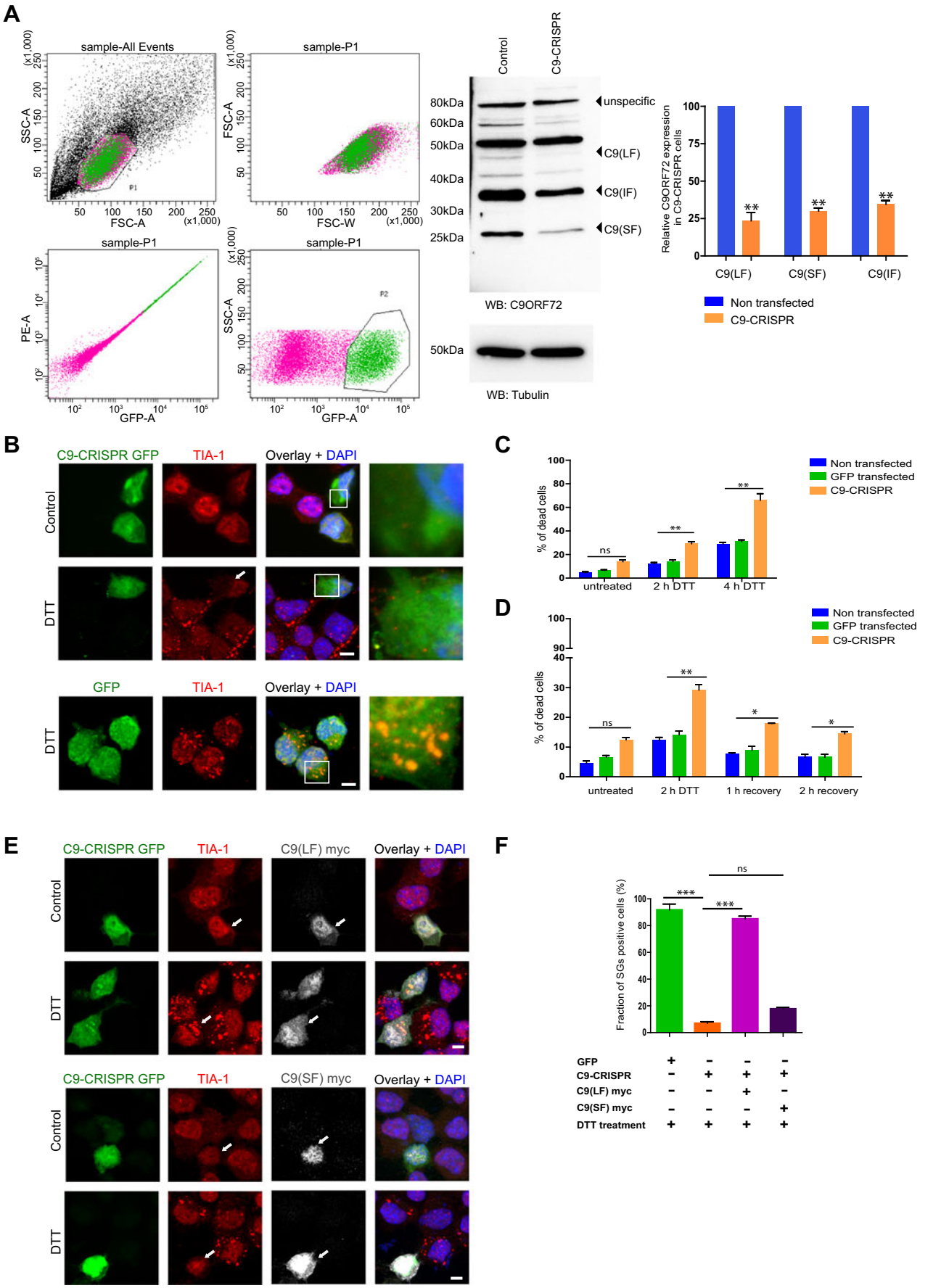
A
sample-All Events
sample-P1
sample-P1
sample-P1
SSC-A
FSC-A
FSC-W
PE-A
GFP-A
P1
P2
Control
C9-CRISPR
80kDa
60kDa
50kDa
40kDa
30kDa
25kDa
unspecific
C9(LF)
C9(IF)
C9(SF)
WB: C9ORF72
50kDa
WB: Tubulin
Relative C9ORF72 expression in C9-CRISPR cells
C9(LF)
C9(SF)
C9(IF)
Non transfected
C9-CRISPR
B
C9-CRISPR GFP
TIA-1
Overlay + DAPI
Control
DTT
GFP
TIA-1
Overlay + DAPI
DTT
C
% of dead cells
Non transfected
GFP transfected
C9-CRISPR
ns
untreated
2 h DTT
4 h DTT
D
% of dead cells
Non transfected
GFP transfected
C9-CRISPR
ns
untreated
2 h DTT
1 h recovery
2 h recovery
E
C9-CRISPR GFP
TIA-1
C9(LF) myc
Overlay + DAPI
Control
DTT
C9-CRISPR GFP
TIA-1
C9(SF) myc
Overlay + DAPI
Control
DTT
F
Fraction of SGs positive cells (%)
ns
GFP
C9-CRISPR
C9(LF) myc
C9(SF) myc
DTT treatment

CRISPR-negative cells, indicating that C9ORF72 is essential for SG formation and might be an important component of SGs (Suppl. Fig. S1a, b). Considering that SG formation is an adaptive physiological response required to surmount cellular stress, we measured the percentage of dead cells in the presence of DTT. By 2 h of DTT exposure, nearly 30 % of C9-CRISPR cells were dead, and this rose significantly to 60 % after 4 h of DTT exposure. In contrast, untransfected and GFP transfected control cells that had retained their capacity to induce SGs in response to stress presented only 30 % cell death after 4 h of DTT exposure (Fig. 5c), thereby demonstrating that the loss of C9ORF72 expression not only impairs SG formation but also hypersensitizes cells to stress and strongly affects cell survival. Next, we analyzed the capacity of cells to recover after stress wherein DTT was washed out after a 2 h treatment period followed by either a 1 or 2 h recovery period. While GFP and untransfected cells had low near-basal levels of cell death after a 2 h recovery period, C9-CRISPR expressing cells presented a significantly higher percentage of cell death (Fig. 5d), suggesting that loss of C9ORF72 expression impairs cellular recovery capacity. Lastly, to pin down the precise role of C9ORF72 in SG formation, a rescue experiment was performed. n2a cells were transfected with C9-CRISPR leading to the knockdown of C9ORF72, followed by a second transfection with C9(LF) myc. DTT exposure now led to robust SG formation in cells, demonstrating that transient C9(LF) myc expression was sufficient to rescue SG formation despite the knockdown of all endogenous C9ORF72 isoforms (Fig. 5e). Further, we examined whether the ability to form SGs was restricted to the C9(LF) isoform or whether other C9ORF72 isoforms had similar physiological functions. Here, we performed the rescue experiment by overexpressing the short isoform of C9ORF72, C9(SF) myc, after C9ORF72 knockdown in n2a cells. Surprisingly, despite the overexpression of C9(SF) myc, cells were unable to regain their ability to induce SGs in response to stress, implying a differential role of the various C9ORF72 isoforms (Fig. 5e).

C9ORF72 Levels Influence Expression of Proteins Critical for SG Formation

Since knockdown of C9ORF72 negatively influenced SG formation, we examined whether C9ORF72 level would affect the expression of other critical proteins involved in SG formation. Protein lysates of C9-CRISPR transfected cells from previous experiment in Fig. 5a were immunoblotted for SG-specific proteins. TIA-1 and HuR levels were drastically reduced upon C9ORF72 knockdown, whereas G3BP1 levels were significantly reduced. However, levels of TDP-43 and FUS/TLS which localize to SGs and are implicated in familial ALS and FTLD remained unchanged between control and knockdown conditions (Fig. 6a). Similar observations were also made via immunostainings, wherein TIA-1 expression levels were reduced while TDP-43 and FUS/TLS expression levels as well as their subcellular localization remained unchanged in C9-CRISPR cells (Fig. 6b). Moreover, the overexpression of C9(LF) myc did not influence the expression levels of both TDP-43 and FUS/TLS, thus ruling out a direct role for C9ORF72 in regulating their expression or localization (Suppl. Fig. S1c, d). Additionally, qPCR revealed that knockdown of C9ORF72 led to a decline in TIA-1 and HuR transcripts, suggesting that C9ORF72 might transcriptionally influence expression levels of other SG-related proteins (Fig. 6c). As further evidence for the involvement of C9ORF72 in the regulation of SG-associated proteins, the transient transfection of C9(LF) myc into C9-CRISPR cells, followed by quantification of mean TIA-1 intensity indicated a near-normal rescue of TIA-1 expression levels. Surprisingly, the transient expression of C9(SF) myc into C9-CRISPR cells did not rescue TIA-1 levels, thereby strengthening the observation that C9(LF) is specifically involved in stress-induced SG formation and also regulates the expression of SG-associated proteins (Fig. 6d).

Fig. 6 C9ORF72 level influences the expression of proteins important for SG formation. **a** Western blot from protein lysates of FACS sorted C9-CRISPR cells presented a reduction in protein levels of TIA-1, HuR, and G3BP1 by approximately 70, 60, and 30 %, respectively, but levels of TDP-43 and FUS/TLS remained unchanged. Results shown are the mean ± SEM of three experiments, *$p<0.05$, **$p<0.01$, ***$p<0.001$. **b** Immunostaining of C9-CRISPR cells shows loss of TIA-1 staining (*arrow*) compared to non-transfected cells, whereas neither change in intensity, nor mislocalization, was observed for TDP-43 and FUS/TLS compared to control cells (*arrow*). **c** qPCR analysis of C9ORF72, TIA-1, and HuR mRNA in n2a cells after transiently transfecting with C9-CRISPR plasmid. Results are presented as fold change compared to control after normalizing with tubulin mRNA. **d** Representative images of n2a cells coexpressing C9-CRISPR and C9(LF) myc or C9(SF) myc plasmid showing the rescue of TIA-1 expression only with C9(LF) myc plasmid (*arrow*). *Right*: Quantitative analysis presenting a significant reduction in TIA-1 intensity in C9-CRISPR transfected cells compared to control cells, and TIA-1 expression level was restored back to normal in C9(LF) myc transfected cells. In contrast, C9(SF) myc failed to restore TIA-1 expression in C9-CRISPR cells. Each value represents the mean ± SEM of 15 cells each from three independent experiments, ***$p<0.001$ (*scale bar* = 4 μm for all image panels)

Expression of Pathogenic Hexanucleotide Expansion Causes Cellular Stress

Lastly, we set out to assess whether the expression of the pathogenic hexanucleotide expansion interferes with the physiological function of normal C9(LF) in SG induction. To do this, we generated various clones containing different GGGGCC repeat expansion in front of full-length C9(LF) myc or GFP (Fig. 7a). Clones containing expansion repeats of $GGGGCC_{(30)}$ and $GGGGCC_{(60)}$ were considered as pathogenic, whereas $GGGGCC_{(3)}$ was taken as normal. We found that the cells transfected with increasing length of pathogenic expansions

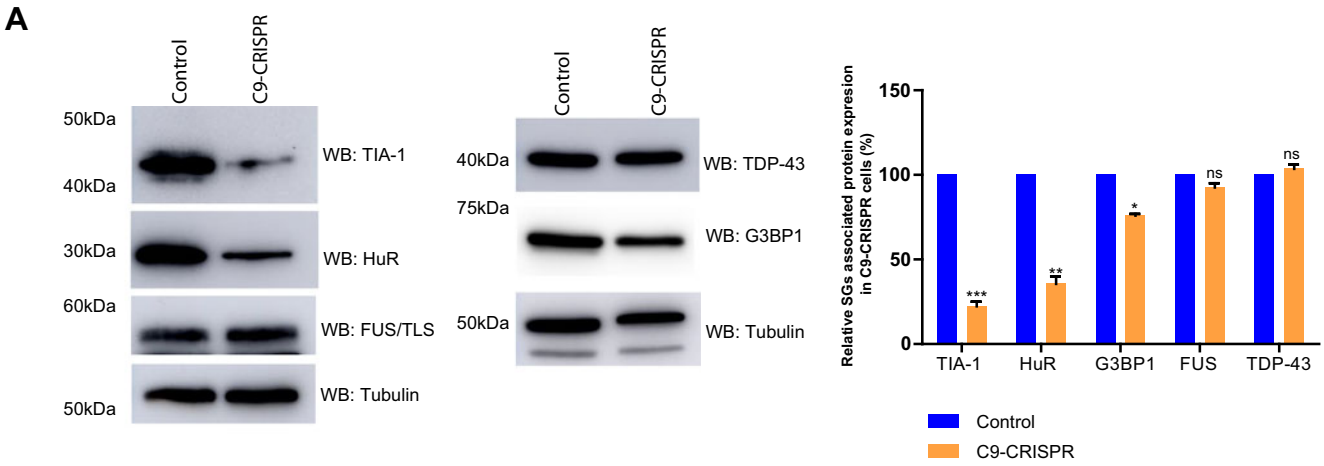

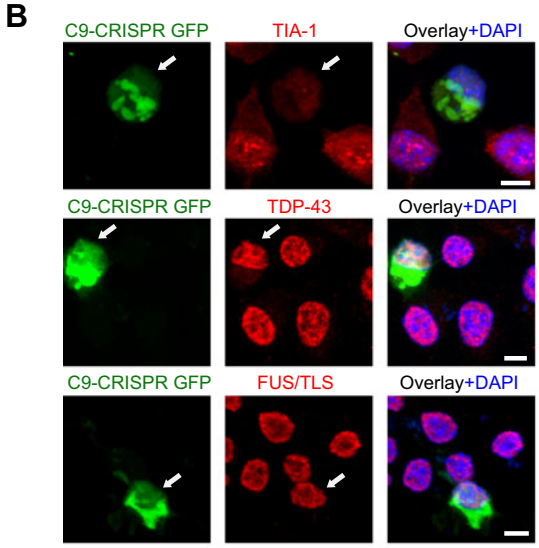

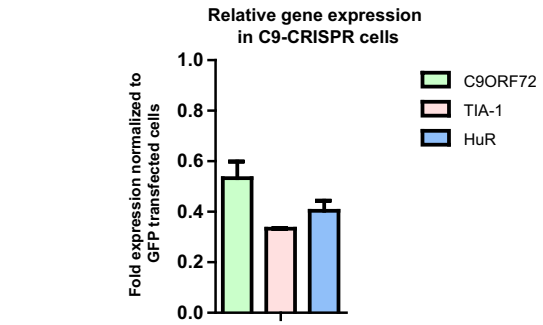

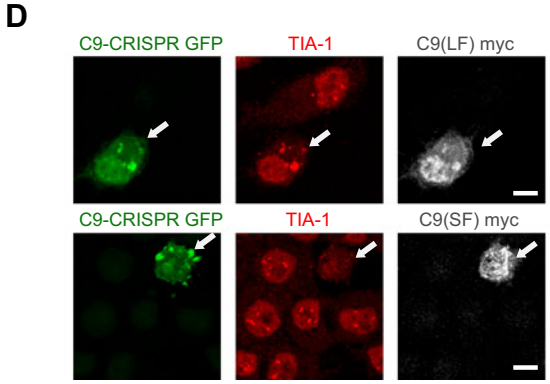

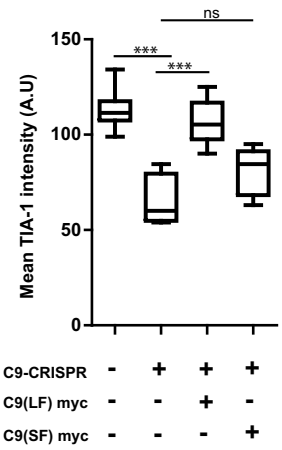

were least efficient in expressing the full-length C9ORF72 and GFP protein (Fig. 7a). We additionally counted the percentage of cells transfected in each condition and found no difference between the percentages of transfected cells in each condition (data not shown), thereby hinting that hexanucleotide expansions might negatively impact protein translation. Interestingly, the expression of the $GGGGCC_{(30)}$-C9(LF) myc and $GGGGCC_{(60)}$-C9(LF) myc but not $GGGGCC_{(3)}$-C9(LF) myc was sufficient to induce the spontaneous appearance of SGs in n2a cells (Fig. 7b, arrows). Similar induction of SGs was also observed in both n2a cells and cortical neurons expressing $GGGGCC_{(30)}$-GFP and $GGGGCC_{(60)}$-GFP indicating that the formation of SGs was repeat length-dependent and equally affected both mitotic and non-mitotic cells (Fig. 7c and

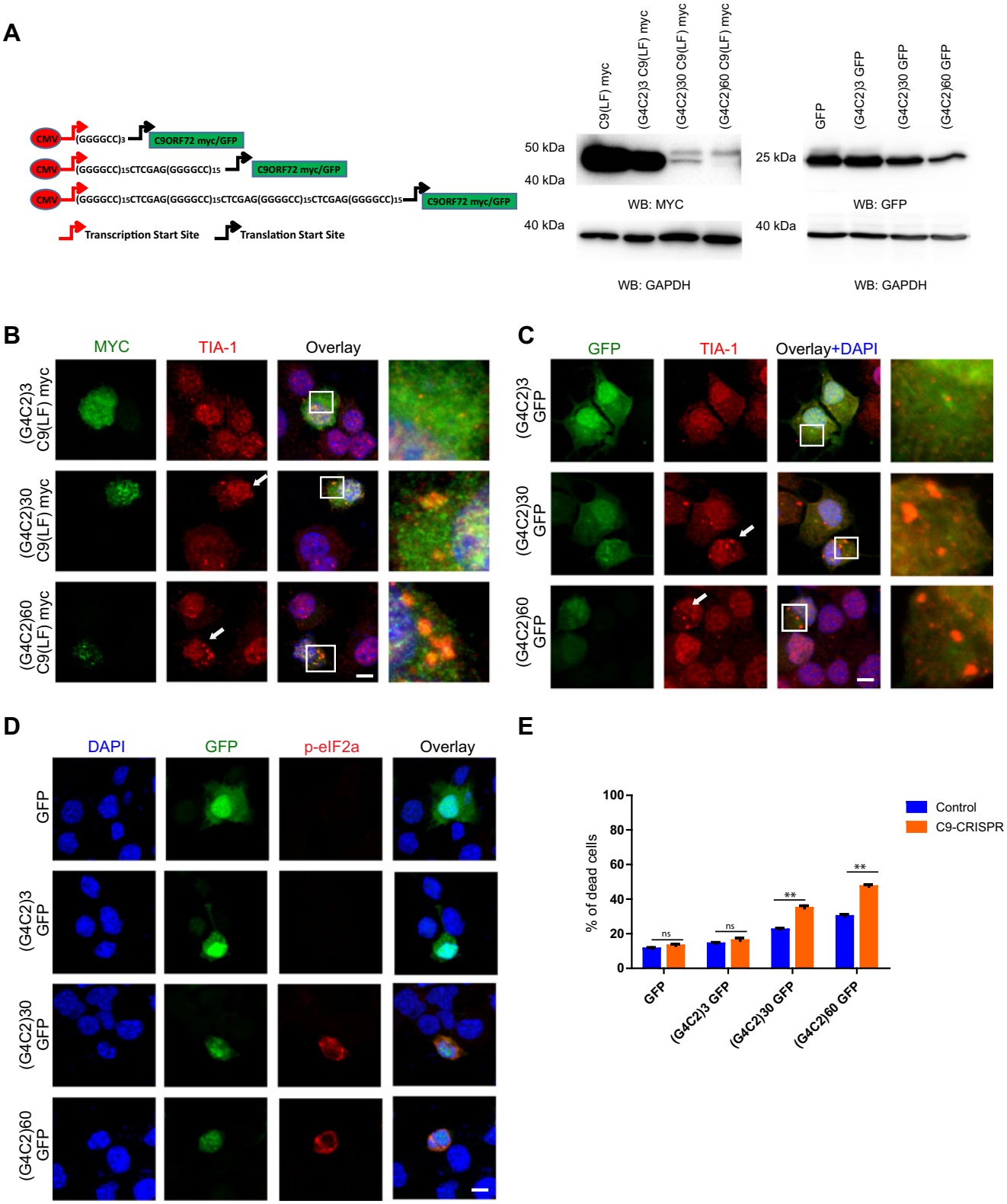

Suppl. Fig. S2). Further, n2a cells expressing $GGGGCC_{(30)}$-GFP and $GGGGCC_{(60)}$-GFP were also strongly positive for phosphorylated eIF2a, confirming that those cytoplasmic puncta were indeed SGs (Fig. 7d).

To examine the reason for SG buildup in cells after transfection of repeat expansions, in situ hybridization (ISH) against the hexanucleotide expansion was performed. Surprisingly, large cytoplasmic granule-like structures

◀ **Fig. 7** Hexanucleotide repeat expansion results in the formation of SGs and impairs cell survival. **a** Schematic representation of pCMV-(GGGGCC)n-C9ORF72 myc and pCMV-(GGGGCC)n GFP constructs. Hexanucleotide repeat expansion was inserted in between the CMV promoter and the ATG start site of C9(LF) myc and GFP constructs. Western blot shows a decrease in the expression of C9ORF72 myc and GFP protein with increasing hexanucleotide repeat lengths. Representative blot from three separate experiments. **b**, **c** 48 h after transfection of n2a cells with constructs having different hexanucleotide repeat lengths were fixed and stained for SGs with TIA-1 antibody. A concomitant increase in number of SGs (*arrows*) was observed with increasing hexanucleotide repeat length, whereas a decline in C9(LF) myc and GFP expression was observed as seen previously via immunoblotting in Fig. 7a. **d** GFP construct with toxic hexanucleotide repeat expansions results in phosphorylation of eIF2a, a prerequisite for SG formation. **e** Dead cells assay reveals an increase in the sensitivity of C9-CRISPR cells to hexanucleotide repeat expansion in comparison to control cells. Each value represents the mean ± SEM from three independent experiments, $^{**}p<0.01$ (*scale bar* = 3 μm for all image panels)

representing RNA foci were observed exclusively in cells expressing the long repeat expansions (Suppl. Fig. S3a). These foci were present within the nucleus (minor fraction) and within the cytoplasm. Besides RNA foci, we examined whether these long repeat expansions also gave rise to dipeptide repeat proteins which have been previously implicated in C9ORF72 pathogenesis. Immunoblotting against dipeptide repeat proteins revealed the presence of these proteins specifically in cells expressing $GGGGCC_{(60)}$-GFP repeats (Suppl. Fig. S3b). These results demonstrate that the hexanucleotide repeat expansions can spontaneously form both toxic RNA foci as well as pathogenic dipeptide repeat proteins, thereby causing cellular stress and impairing C9ORF72 expression. We next mimicked those observations by expressing stress causing hexanucleotide repeat expansions: $GGGGCC_{(30)}$-GFP and $GGGGCC_{(60)}$-GFP, in C9ORF72 knockdown or control cells and examined cellular viability in the presence or absence of endogenous C9ORF72. After 48 h of transfection, we found that C9ORF72 knockout cells were more sensitive to pathogenic hexanucleotide repeat expansion compared to normal cells, suggesting that the lack of C9ORF72 makes cells more sensitive to cellular stress induced by the pathogenic expansions (Fig. 7e). Similarly, expression of GGGGCC(30)-GFP and GGGGCC(60)-GFP in cortical neurons compromised neuronal viability (Suppl. Fig. S3c), indicating that the hexanucleotide repeat expansion associated stress via RNA foci and dipeptide repeat proteins impairs cellular survival responses.

Discussion

Here, we show that normal C9ORF72 is present in P-bodies and upon stress colocalizes within SGs in n2a cells and cortical neurons. Gain of function and loss of function experiments revealed that the long isoform of C9ORF72 is specifically involved in SG formation. CRISPR-mediated knockdown of C9ORF72 completely abolished the assembly of SGs during cellular stress. The loss of C9ORF72 expression also impacted the expression of important proteins required for SG formation such as TIA-1, G3BP1, and HuR, thereby altering the physiological response of the cell to cellular stress. Importantly, loss of C9ORF72 expression compromised the fitness of cells, inducing enhanced and anticipated cell death. Lastly, the expression of the pathological hexanucleotide repeat expansion led to impaired C9ORF72 expression and formation of RNA foci, resulting in prolonged cell stress. Our work identifies a novel role for C9ORF72 in SG formation and sheds light on how pathogenic hexanucleotide repeats might negatively influence normal C9ORF72 expression as well as cause cellular stress due to RNA foci formation and dipeptide repeat proteins. In the context of neurons, this would indicate that the expanded repeats might diminish endogenous C9ORF72 proteins levels thereby impairing neuronal capacity to form SGs during conditions of cellular stress.

The physiological function of C9ORF72 remains unclear, although bioinformatics studies indicated the presence of DENN domain which is prominently present in proteins functioning as guanine nucleotide exchange factors for the Rab GTPases [23, 24]. Moreover, protein interaction studies suggested that C9ORF72 might be involved in a complex associated with autophagosome initiation [25]. Our findings shed novel insights into as yet unknown function of normal C9ORF72 in SG assembly. SGs are cytoplasmic foci that are assembled when cells are exposed to stress, and store mRNAs of housekeeping proteins while allowing the selective translation of stress response proteins, thereby serving as a physiological coping response directed against cellular stress. While normal TDP-43 and FUS/TLS are localized in the nucleus, disease causing mutations accumulate in the cytosol and upon cellular stress both cytosolic TDP-43 and FUS/TLS are associated with TIA-1-positive SGs. Pathological TDP-43 and FUS/TLS inclusions in ALS/FTLD patients contain SG-specific proteins such as PABP-1, suggesting that these inclusions originate from SGs. Moreover, several other proteins like ataxin-2, profilin 1 and survival of motor neuron (SMN), which are causally implicated with motor neuron diseases are also recruited to SGs upon stress conditions, and were shown to regulate SG dynamics [26–28]. Interestingly, valosin-containing protein (VCP) is involved in the autophagic clearance of SGs and inhibiting its normal function impairs SG formation, morphology and composition [29]. Recent studies have strongly implicated altered SG dynamics in ALS/FTLD. Moreover, previous evidences from C9ORF72 patients presenting inclusions positive for TDP-43, and poly-A binding protein as well as the interaction of C9ORF72 with RNA binding proteins like hnRNPs [30, 31] indicate a probable association with SGs.

Here, we provide evidence that normal C9ORF72 is present within P-bodies and is critically involved in maintaining SG assembly during cellular stress responses and indirectly maintains cell fitness. Since SG formation is a protective mechanism, neurons that retain the capacity to mount an efficient stress response via the transient formation of SGs followed by recovery of translation are protected from ischemia-related cell death [32]. However, as with most stress responses, initial neuroprotective effects are replaced by toxic effects when SG pathway is either hyperactive or chronic translation repression persists. Our finding that the knockdown of C9ORF72 inhibits SG assembly, thereby making cells hypersensitive to stressors such as ER stress, suggests that C9ORF72 has an important role in maintaining adaptive stress responses and influences cell survival. In *Caenorhabditis elegans*, the knockdown of C9ORF72 orthologue resulted in strains being hypersensitive to osmotic stress which eventually aggravated motor neuron degeneration [33]. Further, the presence of hexanucleotide expansion repeats negatively impact protein expression, thereby mimicking a knockdown situation and eventually inhibiting cellular SG assembly during stress. Similarly, reduced expression of C9ORF72 has been observed in postmortem cortical tissue of ALS and FTLD patients with hexanucleotide repeat expansion in lymphoblastoid cell lines and in neurons derived from induced pluripotent stem cell (iPSC) lines [10–12, 18, 34]. The knockdown of the zebrafish orthologue; zC9orf72 expression leads to axonal degeneration of motor neurons [35]. Although, presently it is unclear whether the loss of function of C9ORF72 is causally associated with the pathology, as other studies wherein C9ORF72 was knocked down in mouse using anti-sense oligonucleotides did not produce any degenerative phenotype [36], an indirect role for the loss of function of C9ORF72 in the development of ALS pathogenesis cannot be ruled out.

Recent studies have identified that the non-ATG (RAN) translation of hexanucleotide repeats from sense and antisense transcripts accumulates in C9ORF72-associated ALS/FTD patient tissues [11, 13], suggesting a probable pathogenic role for these proteins. Furthermore, dipeptide repeat proteins or RAN-translated proteins were shown to be toxic and involved in disease-associated pathology [37–39]. Interestingly, from the five dipeptide repeat proteins, poly-arginine (GR) and poly-proline-arginine (PR) selectively localized to the nucleolus and caused nucleolar stress and cell death due to inhibition of ribosomal RNA synthesis and impairment of SG formation [40, 41]. Similarly, we have found that in n2a and cortical neurons which expressed normal C9ORF72 proteins, the exogenous expression of constructs containing pathogenic hexanucleotide repeats in front of C9ORF72 or GFP induced spontaneous SGs. However, when the same constructs were expressed in C9-CRISPR cells, then cells had compromised their ability to assemble SGs, which was reflected by the accelerated cell death. This implies that in in vivo condition long hexanucleotide repeats might impair C9ORF72 expression and simultaneously induce stress by the formation of dipeptide repeat proteins, which in turn can negatively influence SG assembly. The precise contribution of both reduced C9ORF72 expression and dipeptide repeat proteins in impairing SG assembly needs further investigation.

Furthermore, hexanucleotide expansions in the first intron of C9ORF72 also lead to the formation and accumulation of RNA foci [10] which have been observed in patient cells. Transgenic mice with normal human C9ORF72 gene or disease-associated expansions replicated the disease-associated pathology seen in C9ORF72-associated ALS patients, such as the presence of extensive RNA foci and dipeptide repeat proteins [42, 43]. Similar RNA inclusions have been found in Huntington's disease like-2, fragile X-associated tremor ataxia syndrome, and spinocerebellar ataxias 8, 10, and 31. Of note, all these neurodegenerative diseases involve abnormally long repeat expansions such as CUG, CCUG, CGG, CAG, AUUCU, and UGGAA which accumulate as RNA foci. Our work revealed that long hexanucleotide repeat expansions in C9ORF72 gene not only forms RNA foci but also induces stress as revealed by the presence of SGs. These toxic foci can sequester both RNA as well as RNA binding proteins critical for the functioning of the cell. Notably, in C9ORF72 transgenic mice, both RNA foci and dipeptide repeat proteins were not sufficient to induce neurodegeneration until late ages, suggesting the requirement of yet another factor such as the loss of function of the normal C9ORF72 gene in the neurodegenerative process [42, 43]. In this regard, our study indicates that the stress imposed by the accumulation of RNA foci and dipeptide repeat proteins coupled together with reduced C9ORF72 expression due to hexanucleotide repeat expansions impairs the relevant SG formation, thereby compromising cellular adaptive and survival responses. Further, we reveal a novel function for normal long isoform of C9ORF72 in stress-associated SG assembly and cellular recovery.

Acknowledgments This work was supported by the Synapsis Foundation, Frick foundation for ALS research, and Swiss National Science Foundation Professorship grant (150756), to S.S. We thank Gabor Morotz, Kings College London, UK, for help with cortical neuron cultures.

References

1. Rowland L, Shneider N (2001) Amyotrophic lateral sclerosis. N Engl J Med 344:1688–1700. doi:10.1056/NEJM200105313442207
2. Ratnavalli E, Brayne C, Dawson K, Hodges JR (2002) The prevalence of frontotemporal dementia. Neurology 58:1615–1621
3. Liscic RM, Storandt M, Cairns NJ, Morris JC (2007) Clinical and psychometric distinction of frontotemporal and Alzheimer dementias. Arch Neurol 64:535–540

4. Phukan J, Pender NP, Hardiman O (2007) Cognitive impairment in amyotrophic lateral sclerosis. Lancet Neurol 6(11):994–1003
5. Giordana MT, Ferrero P, Grifoni S, Pellerino A, Naldi A, Montuschi A (2011) Dementia and cognitive impairment in amyotrophic lateral sclerosis: a review. Neurol Sci 32:9–16. doi:10.1007/s10072-010-0439-6
6. Lomen-Hoerth C, Anderson T, Miller B. The overlap of amyotrophic lateral sclerosis and frontotemporal dementia. Neurology. 2002. pp. 1077–1079. doi:10.1212/WNL.59.7.1077
7. Neumann M, Roeber S, Kretzschmar H a, Rademakers R, Baker M, Mackenzie IR a (2009) Abundant FUS-immunoreactive pathology in neuronal intermediate filament inclusion disease. Acta Neuropathol 118:605–616. doi:10.1007/s00401-009-0581-5
8. Neumann M, Sampathu DM, Kwong LK, Truax AC, Micsenyi MC, Chou TT, Bruce J, Schuck T et al (2006) Ubiquitinated TDP-43 in frontotemporal lobar degeneration and amyotrophic lateral sclerosis. Science 314:130–3. doi:10.1126/science.1134108
9. Renton AE, Majounie E, Waite A, Simón-Sánchez J, Rollinson S, Gibbs JR, Schymick JC, Laaksovirta H et al (2011) A hexanucleotide repeat expansion in C9ORF72 is the cause of chromosome 9p21-linked ALS-FTD. Neuron 72:257–68. doi:10.1016/j.neuron.2011.09.010
10. DeJesus-Hernandez M, Mackenzie IR, Boeve BF, Boxer AL, Baker M, Rutherford NJ, Nicholson AM, Finch NA et al (2011) Expanded GGGGCC hexanucleotide repeat in noncoding region of C9ORF72 causes chromosome 9p-linked FTD and ALS. Neuron 72:245–256. doi:10.1016/j.neuron.2011.09.011
11. Mori K, Weng S-M, Arzberger T, May S, Rentzsch K, Kremmer E, Schmid B, Kretzschmar HA et al (2013) The C9orf72 GGGGCC repeat is translated into aggregating dipeptide-repeat proteins in FTLD/ALS. Science 339:1335–8. doi:10.1126/science.1232927
12. Gijselinck I, Van Langenhove T, van der Zee J, Sleegers K, Philtjens S, Kleinberger G, Janssens J, Bettens K et al (2012) A C9orf72 promoter repeat expansion in a Flanders-Belgian cohort with disorders of the frontotemporal lobar degeneration-amyotrophic lateral sclerosis spectrum: a gene identification study. Lancet Neurol 11:54–65
13. Ash PE a, Bieniek KF, Gendron TF, Caulfield T, Lin W-L, Dejesus-Hernandez M, van Blitterswijk MM, Jansen-West K et al (2013) Unconventional translation of C9ORF72 GGGGCC expansion generates insoluble polypeptides specific to c9FTD/ALS. Neuron 77:639–646. doi:10.1016/j.neuron.2013.02.004
14. Mackenzie IR, Arzberger T, Kremmer E, Troost D, Lorenzl S, Mori K, Weng SM, Haass C et al (2013) Dipeptide repeat protein pathology in C9ORF72 mutation cases: clinico-pathological correlations. Acta Neuropathol 126:859–79. doi:10.1007/s00401-013-1181-y
15. Farg MA, Sundaramoorthy V, Sultana JM, Yang S, Atkinson RAK, Levina V, Halloran MA, Gleeson PA et al (2014) C9ORF72, implicated in amytrophic lateral sclerosis and frontotemporal dementia, regulates endosomal trafficking. Hum Mol Genet 23:3579–3595. doi:10.1093/hmg/ddu068
16. Xu Z, Poidevin M, Li X, Li Y, Shu L, Nelson DL, Li H, Hales CM et al (2013) Expanded GGGGCC repeat RNA associated with amyotrophic lateral sclerosis and frontotemporal dementia causes neurodegeneration. Proc Natl Acad Sci U S A 110:7778–83. doi:10.1073/pnas.1219643110
17. Strober W. Trypan blue exclusion test of cell viability. Curr Protoc Immunol. 2001;Appendix 3: Appendix 3B. doi:10.1002/0471142735.ima03bs21
18. Waite AJ, Bäumer D, East S, Neal J, Morris HR, Ansorge O, Blake DJ (2014) Reduced C9orf72 protein levels in frontal cortex of amyotrophic lateral sclerosis and frontotemporal degeneration brain with the C9ORF72 hexanucleotide repeat expansion. Neurobiol Aging 35:1779.e5–1779.e13. doi:10.1016/j.neurobiolaging.2014.01.016
19. Wilczynska A, Aigueperse C, Kress M, Dautry F, Weil D (2005) The translational regulator CPEB1 provides a link between dcp1 bodies and stress granules. J Cell Sci 118:981–992
20. Kedersha N, Stoecklin G, Ayodele M, Yacono P, Lykke-Andersen J, Fitzler MJ, Scheuner D, Kaufman RJ et al (2005) Stress granules and processing bodies are dynamically linked sites of mRNP remodeling. J Cell Biol 169:871–884
21. Anderson P, Kedersha N (2006) RNA granules. J Cell Biol 172:803–808
22. Kedersha N, Anderson P (2002) Stress granules: sites of mRNA triage that regulate mRNA stability and translatability. Biochem Soc Trans 30:963–969
23. Zhang D, Iyer LM, He F, Aravind L. Discovery of Novel DENN Proteins: Implications for the Evolution of Eukaryotic Intracellular Membrane Structures and Human Disease. Front Genet. 2012;3. doi:10.3389/fgene.2012.00283
24. Levine TP, Daniels RD, Gatta AT, Wong LH, Hayes MJ (2013) The product of C9orf72, a gene strongly implicated in neurodegeneration, is structurally related to DENN Rab-GEFs. Bioinformatics 29:499–503. doi:10.1093/bioinformatics/bts725
25. Behrends C, Sowa ME, Gygi SP, Harper JW (2010) Network organization of the human autophagy system. Nature 466:68–76
26. Nonhoff U, Ralser M, Welzel F, Piccini I, Balzereit D, Yaspo M, Lehrach H, Krobitsch S (2007) Ataxin-2 interacts with the DEAD/H-box RNA helicase DDX6 and interferes with P-bodies and stress granules. Mol Biol Cell 18:1385–96. doi:10.1091/mbc.E06-12-1120
27. Figley MD, Bieri G, Kolaitis R-M, Taylor JP, Gitler AD (2014) Profilin 1 associates with stress granules and ALS-linked mutations alter stress granule dynamics. J Neurosci 34:8083–97. doi:10.1523/JNEUROSCI.0543-14.2014
28. Zou T, Yang X, Pan D, Huang J, Sahin M, Zhou J (2011) SMN deficiency reduces cellular ability to form stress granules, sensitizing cells to stress. Cell Mol Neurobiol 31:541–50. doi:10.1007/s10571-011-9647-8
29. Seguin SJ, Morelli FF, Vinet J, Amore D, De Biasi S, Poletti A, Rubinsztein DC, Carra S (2014) Inhibition of autophagy, lysosome and VCP function impairs stress granule assembly. Cell Death Differ. Nat Publ Group 21:1838–1851. doi:10.1038/cdd.2014.103
30. Cooper-Knock J, Walsh MJ, Higginbottom A, Highley JR, Dickman MJ, Edbauer D, Ince PG, Wharton SB et al (2014) Sequestration of multiple RNA recognition motif-containing proteins by C9orf72 repeat expansions. Brain 137:2040–2051. doi:10.1093/brain/awu120
31. McGurk L, Lee VM, Trojanowksi JQ, Van Deerlin VM, Lee EB, Bonini NM (2014) Poly-a binding protein-1 localization to a subset of TDP-43 inclusions in amyotrophic lateral sclerosis occurs more frequently in patients harboring an expansion in C9orf72. J Neuropathol Exp Neurol 73(9):837–845. doi:10.1097/NEN.0000000000000102
32. Jamison JT, Kayali F, Rudolph J, Marshall M, Kimball SR, DeGracia DJ (2008) Persistent redistribution of poly-adenylated mRNAs correlates with translation arrest and cell death following global brain ischemia and reperfusion. Neuroscience 154:504–520
33. Therrien M, Rouleau G a, Dion P a, Parker JA (2013) Deletion of C9ORF72 results in motor neuron degeneration and stress sensitivity in *C. elegans*. PLoS One 8, e83450. doi:10.1371/journal.pone.0083450
34. Almeida S, Gascon E, Tran H, Chou HJ, Gendron TF, Degroot S, Tapper AR, Sellier C et al (2013) Modeling key pathological features of frontotemporal dementia with C9ORF72 repeat expansion in iPSC-derived human neurons. Acta Neuropathol 126:385–399
35. Ciura S, Lattante S, Le Ber I, Latouche M, Tostivint H, Brice A, Kabashi E (2013) Loss of function of C9orf72 causes motor deficits in a zebrafish model of amyotrophic lateral sclerosis. Ann Neurol 74:180–187

36. Lagier-Tourenne C, Baughn M, Rigo F, Sun S, Liu P, Li H-R, Jiang J, Watt AT et al (2013) Targeted degradation of sense and antisense C9orf72 RNA foci as therapy for ALS and frontotemporal degeneration. Proc Natl Acad Sci U S A 110:E4530–9. doi:10.1073/pnas.1318835110
37. Mizielinska S, Grönke S, Niccoli T, Ridler CE, Clayton EL, Devoy A, Moens T, Norona FE et al (2014) C9orf72 repeat expansions cause neurodegeneration in Drosophila through arginine-rich proteins. Science 345:1192–1194. doi:10.1126/science.1256800
38. Zhang Y-J, Jansen-West K, Xu Y-F, Gendron TF, Bieniek KF, Lin W-L, Sasaguri H, Caulfield T et al (2014) Aggregation-prone c9FTD/ALS poly(GA) RAN-translated proteins cause neurotoxicity by inducing ER stress. Acta Neuropathol 128:505–524. doi:10.1007/s00401-014-1336-5
39. Kwon I, Xiang S, Kato M, Wu L, Theodoropoulos P, Wang T, Kim J, Yun J et al (2014) Poly-dipeptides encoded by the C9ORF72 repeats bind nucleoli, impede RNA biogenesis, and kill cells. Science 345:1254917. doi:10.1126/science.1254917
40. Wen X, Tan W, Westergard T, Krishnamurthy K, Markandaiah SS, Shi Y, Lin S, Shneider NA et al (2014) Antisense proline-arginine RAN dipeptides linked to C9ORF72-ALS/FTD form toxic nuclear aggregates that initiate in vitro and in vivo neuronal death. Neuron 84:1213–1225. doi:10.1016/j.neuron.2014.12.010
41. Tao Z, Wang H, Xia Q, Li K, Li K, Jiang X, Xu G, Wang G et al (2015) Nucleolar stress and impaired stress granule formation contribute to C9orf72 RAN translation-induced cytotoxicity. Hum Mol Genet 24:2426–41. doi:10.1093/hmg/ddv005
42. Peters OM, Cabrera GT, Tran H, Gendron TF, McKeon JE, Metterville J, Weiss A, Wightman N et al (2015) Human C9ORF72 hexanucleotide expansion reproduces RNA foci and dipeptide repeat proteins but not neurodegeneration in BAC transgenic mice. Neuron Elsevier Ltd 88:902–909. doi:10.1016/j.neuron.2015.11.018
43. O'Rourke JG, Bogdanik L, Muhammad AKMG, Gendron TF, Kim KJ, Austin A, Cady J, Liu EY et al (2015) C9orf72 BAC transgenic mice display typical pathologic features of ALS/FTD. Neuron 88:892–901. doi:10.1016/j.neuron.2015.10.027